

Lawrence Berkeley National Laboratory

Recent Work

Title

Strong One-Dimensional Characteristics of Hole-Carriers in ReS₂ and ReSe₂.

Permalink

<https://escholarship.org/uc/item/2kp0t8jr>

Journal

Scientific reports, 9(1)

ISSN

2045-2322

Authors

Kim, BS
Kyung, WS
Denlinger, JD
et al.

Publication Date

2019-02-01

DOI

10.1038/s41598-019-39540-4

Peer reviewed

SCIENTIFIC REPORTS

OPEN

Strong One-Dimensional Characteristics of Hole-Carriers in ReS_2 and ReSe_2

B. S. Kim^{1,2,3}, W. S. Kyung^{1,2,4}, J. D. Denlinger⁴, C. Kim^{1,2} & S. R. Park³

Each plane of layered ReS_2 and ReSe_2 materials has 1D chain structure, from which intriguing properties such as 1D character of the exciton states and linearly polarized photoluminescence originate. However, systematic studies on the 1D character of charge carriers have not been done yet. Here, we report on systematic and comparative studies on the energy-momentum dispersion relationships of layered transition metal dichalcogenides ReS_2 and ReSe_2 by angle resolved photoemission. We found that the valence band maximum or the minimum energy for holes is located at the high symmetric Z-point for both materials. However, the out-of-plane (k_z) dispersion for ReSe_2 (20 meV) is found to be much smaller than that of ReS_2 (150 meV). We observe that the effective mass of the hole carriers along the direction perpendicular to the chain is about 4 times larger than that along the chain direction for both ReS_2 and ReSe_2 . Remarkably, the experimentally measured hole effective mass is about twice heavier than that from first principles calculation for ReS_2 although the in-plane anisotropy values from the experiment and calculations are comparable. These observation indicate that bulk ReS_2 and ReSe_2 are unique semiconducting transition metal dichalcogenides having strong one-dimensional characters.

Layered transition-metal dichalcogenides (TMDs) have been extensively studied in recent years because of their potential as electronic materials for future devices. Their intriguing characters of the electronic structures such as the valley degeneracy¹ and spin-valley-layer locking^{2–4}, provide added value for valley- and spintronic applications. While some of them even exhibit superconductivity and charge density waves originating from the electron-phonon and electron-electron interactions due to their low electronic dimensionality (e.g. in NbSe_2 ^{5,6}), most of the studies have been focused on Mo and W compounds due to their semi-conducting properties and close to ideal 2 dimensionality^{7–11}.

Very recently, layered ReS_2 and ReSe_2 began to draw attention as their layer-layer interactions are much weaker than other layered TMDs¹². More interestingly, ReS_2 and ReSe_2 have one-dimensional (1D) characters in their structure as well as optical and electrical properties due to the formation of Re chain structure stemming from the distortion in the 1T structural phase^{12–14}. High-resolution transmission electron microscopy and electron diffraction studies reveal distorted 1T structure with Re chain formation¹². Such structure distortion is directly related to the high anisotropy in the Raman response from in-plane lattice vibrations^{14–19}. It also affects optical properties, e.g., anisotropic character in optical absorption or photoluminescence comes from that of excitons^{20–24}. Electrical conductivity is also found to be much higher along the chain direction than the direction perpendicular to the chain^{13,25,26}.

As the above-mentioned intriguing 1D properties are determined by the characteristics of hole and electron band dispersions, electronic structure studies by angle resolved photoemission spectroscopy (ARPES) are naturally desired. Especially, the effective mass is a fundamental parameter that can be obtained from the energy and momentum dispersion relationship and governs the electrical and optical properties such as mobility, conductivity, light absorption and photoluminescence. In fact, a couple of ARPES studies on ReS_2 and ReSe_2 have been reported and the results indicate an in-plane anisotropy in the hole band dispersion as expected from the chain structures in ReS_2 ^{27–29} and in ReSe_2 ³⁰. However, obtaining very high-quality data needed to determine the effective mass for all directions turned out to be challenging. For example, the photon energy dependence of the

¹Department of Physics and Astronomy, Seoul National University, Seoul, 08826, Korea. ²Center for Correlated Electron Systems, Institute for Basic Science, Seoul, 08826, Korea. ³Department of Physics, Incheon National University, Incheon, 22012, Korea. ⁴Advanced Light Source, Lawrence Berkeley National Laboratory, Berkeley, CA, 94720, USA. Correspondence and requests for materials should be addressed to C.K. (email: changyoung@snu.ac.kr) or S.R.P. (email: AbePark@inu.ac.kr)

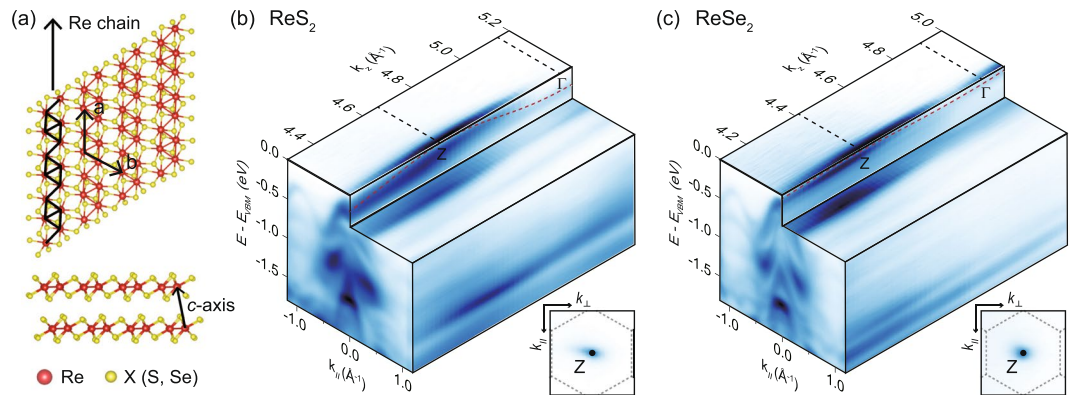


Figure 1. Crystal structure and out-of-plane valence band dispersions. **(a)** Top and side views of the crystal structure of ReX_2 ($X = \text{S}, \text{Se}$). It shows distorted 1T structure with Re chains indicated by black solid lines. **(b,c)** Intensity plots of ReS_2 and ReSe_2 ARPES data in the energy and momentum space, respectively. k_z dependent intensities are taken by using different photon energies from 60 eV to 110 eV with 2 eV step. k_z is obtained with inner potentials of 17.8 and 12.4 eV for ReS_2 and ReSe_2 , respectively. k_{\parallel} and k_{\perp} are in-plane momentum parallel and perpendicular to the chain, respectively. Red dashed lines are guides to eye for k_z dispersion of the top-most valence bands. Insets are 2D constant energy ($E = E_{\text{VBM}}$) intensity map in the momentum-space (as functions of k_{\parallel} and k_{\perp}) at the $k_z = \text{Z}$ -point. Note that there is a single peak at the zero in-plane momentum point (Z-point).

valence band dispersion for ReS_2 appears to be very different among the reported results^{27,29}. In addition, direct comparison between measured valence band dispersions of ReS_2 and ReSe_2 , for which lattice parameters are quite different³¹, are difficult because the data were taken in different Brillouin zones for ReS_2 and ReSe_2 ^{29,30}.

In order to resolve aforementioned issues, we have performed systematic ARPES studies on ReS_2 and ReSe_2 . Our goal is to take data for the entire momentum space which is good enough to do quantitative analysis and obtain in-plane anisotropy in the effective hole mass for the two materials for a comparative study. Our data show a striking difference from what were reported in previous experimental and theoretical studies^{29,30,32}. (1) The valence band maximum (VBM) is located at the Z-point for both systems, while it was reported in a previous ARPES study reported that VBM of ReSe_2 may be located at non-high-symmetric momentum point^{30,33}. (2) The k_z dispersion of ReSe_2 is much smaller than that of published quasiparticle band structure within the LDA + *GdW* approximation³². (3) The effective hole masses along and perpendicular to the chain direction are quite different from the reported experimental and theoretical values^{29,30,34}.

Results and Discussion

Valence band maximum of ReSe_2 and ReS_2 . ReS_2 and ReSe_2 are layered materials in which the van der Waals interaction between layers is extremely weak, even weaker than other TMDs¹². The crystal structure for both ReS_2 and ReSe_2 is the so-called distorted 1T structure. Re atoms show a hexagonal network but the structure is distorted to have chain structures as indicated by black lines in Fig. 1(a). The 1D chain structure makes these materials unique among TMDs in that optical and electrical properties carry 1D characteristics^{14–26}.

The inner potential can be estimated from the k_z dispersion of electronic band (Fig. 1(b) and (c)) with the reciprocal lattice vector \mathbf{c}^* . Based on the results of reported X-ray diffraction measurements³¹, the reciprocal lattice vector \mathbf{c}^* is calculated to be 1.032 \AA^{-1} (0.984 \AA^{-1}) for ReS_2 (ReSe_2). The inner potential is estimated to be $V_0 = 17.8$ and 12.4 eV for ReS_2 and ReSe_2 . These estimated values are similar to those of other TMDs^{35,36}.

ARPES experiments are performed on ReS_2 and ReSe_2 to obtain the energy-and-momentum dispersion of the hole carriers. ARPES intensities as a function of the energy referenced to the valence band maximum (E_{VBM}) are mapped along two momentum directions, parallel to chain (k_{\parallel}) and perpendicular to the layer (k_z) (Fig. 1(b,c)). While several band dispersions are observed within the energy range, the top-most valence band is of interest as it determines the low energy properties of the materials such as electrical conductivity. Due to the layered structure, the top-most bands of ReS_2 and ReSe_2 show relatively weak dispersions along k_z than along in-plane momentum. Interestingly, we observed as shown in Fig. 1 that the k_z dispersion of ReSe_2 (about 20 meV) is even weaker compared to that of ReS_2 (about 150 meV) which is known as a material with very weak inter-layer interaction¹². Therefore, our results show an evidence for even smaller interaction between layers in ReSe_2 .

Our photon energy dependence data reveal that VBM is located at Z for both ReS_2 and ReSe_2 as indicated by the red dashed lines in Fig. 1(b,c). While previous ARPES studies also showed that VBM of ReS_2 is located at Z, VBM of ReSe_2 has been under debate. Hart *et al.* reported that the k_z for VBM of ReSe_2 is the same as the Z-point but the in-plane momentum was reported to be non-zero³⁰. More recently, Eickholt *et al.* reported two VBM of ReSe_2 ³³. One of them is at Z and the other is away from Z. But their experiment could not decide which is global VBM, since data quality is not good enough. The global VBM of ReSe_2 can be decided to be located at Z due to high quality data. Please refer to the supplementary materials for more details. In fact, we find that ReSe_2 result about VBM is consistent with a recent theoretical prediction as well³².

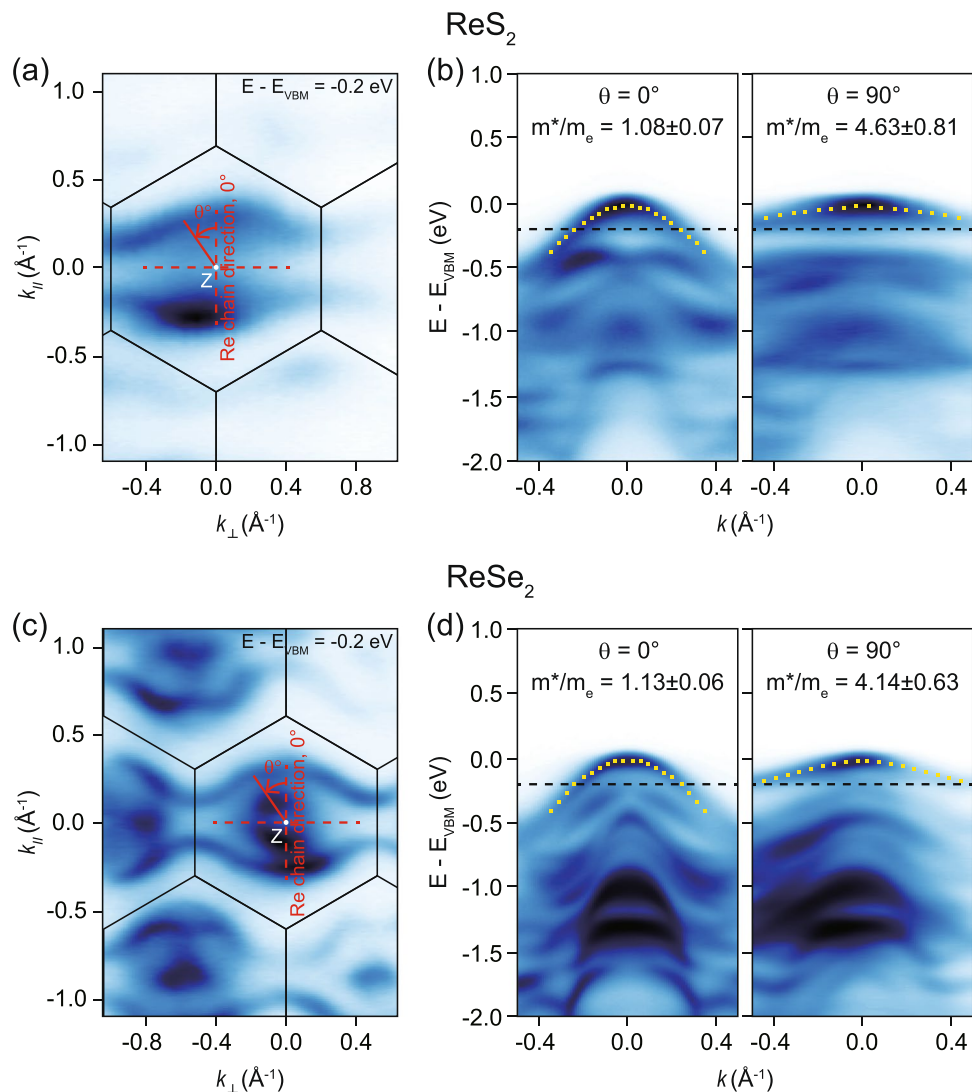


Figure 2. In-plane valence band dispersions near the valence band maximum. Constant energy ($E - E_{\text{VBM}} = -0.2$ eV) ARPES maps of ReS_2 (a) and ReSe_2 (c). The photon energy used for the experiment was 70 eV for ReS_2 and 68 eV for ReSe_2 . For these photon energies, $k_z = \text{Z point}$ (white dot) where VBM is located is included in the data. Red solid and dashed lines in (a,c) indicate the direction parallel and perpendicular to the Re chain direction, respectively. θ is defined as the relative angle from the direction along the chain as shown in the figure. The honey comb structured line indicates the projected Brillouin zone boundary. (b,d) High symmetric cuts along ($\theta = 0^\circ$) and perpendicular ($\theta = 90^\circ$) to the Re chain. The dotted lines in (b,d) are quadratic fit to the top-most bands. The effective masses of hole carriers of ReX_2 extracted from the fitting functions are shown in the figures.

Directional dependence of effective hole masses in ReS_2 and ReSe_2 . In order to investigate the effective mass of the hole carrier, we analyze ARPES data obtained in the in-plane momentum space that includes the Z-point. As shown in Fig. 2(a,c), constant energy maps of ARPES intensities of ReS_2 and ReSe_2 at $E - E_{\text{VBM}} = -0.2$ eV show two-fold symmetry and strong anisotropic band contours which are not closed along the direction perpendicular to the chain. These observations indicate much smaller band dispersion along the direction perpendicular to the chain. The top-most band dispersions, which we are interested in, along the chain are much stronger than those along the other for both ReS_2 and ReSe_2 . For quantitative analysis, we try to fit the band dispersions with a quadratic function for which the effective mass is a free parameter³². The dotted lines in Fig. 2(b,d) indicate the fit functions. So, obtained effective masses along the direction perpendicular to the chain ($4.63 m_e$ for ReS_2 and $4.14 m_e$ for ReSe_2) are much heavier than the effective masses along chain ($1.08 m_e$ for ReS_2 and $1.13 m_e$ for ReSe_2). That is, the effective mass along the chain is about 4 times lighter than that perpendicular to the chain for both ReS_2 and ReSe_2 . This in-plane anisotropy value in the effective hole mass is the largest among semiconducting TMDs^{37,38}.

The valence band dispersion can also be analyzed for different theta angle and corresponding effective hole mass can be obtained. Shown in Fig. 3(a,b) are ARPES data along in-plane momentum set by the θ angle defined in Fig. 2(a). The data are subsequently analyzed and the corresponding effective hole mass is obtained for a

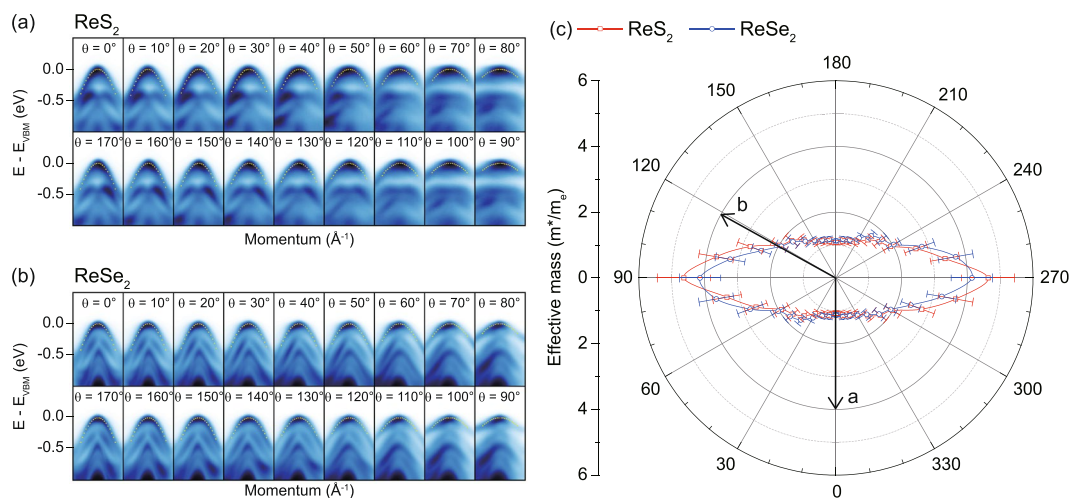


Figure 3. Anisotropic effective hole masses. ARPES cut data along the in-plane momentum defined by the angle θ (see Fig. 2(a) for definition) for (a) ReS₂ and (b) ReSe₂. All the data sets are centered around the Z-point at which VBM is located. The dotted lines indicate a quadratic function fitting the dispersions of the top-most bands. The effective mass from the quadratic fit function for each angle can be extracted and is plotted for ReS₂ and ReSe₂ in (c). Arrows indicate crystallographic orientation of ReX₂.

systematic study of direction dependence. We notice the top-most band can be fitted well with a quadratic function indicated by dotted lines, which makes us confident in our analysis. The extracted effective mass from the quadratic function is plotted in polar coordinate as a function of the theta angle in Fig. 3(c). The plot clearly shows two-fold symmetry and strong in-plane anisotropy of the effective hole mass for both ReS₂ (red) and ReSe₂ (blue). There is an important point to discuss in comparison with the results of first principles calculations on ReS₂. The experimentally observed effective mass is about twice larger than that from the first principles calculations. The effective mass from the first principles calculations is $2.4 m_e$ along the direction perpendicular to the chain and $0.8 m_e$ along the chain²⁷. The electron-electron and electron-phonon interactions or atomic spin-orbit coupling of Re atom which were not considered in the calculation may play a crucial role in the clear enhancement of the effective hole mass.

Conclusions

In this study, we performed systematic ARPES studies of ReS₂ and ReSe₂ to reveal the energy-momentum dispersion relationships of the top most valence bands. We found that ReSe₂ have much smaller k_z dispersion than ReS₂, indicating the more 2D-like feature in ReSe₂ than in ReS₂. We systematically investigated in-plane directional dependence of the effective hole masses of ReS₂ and ReSe₂. The effective masses show strong anisotropy, about 4 times lighter along the chain than the direction perpendicular to the chain. In-plane anisotropy of the hole effective masses in ReS₂ and ReSe₂ is larger than that in black phosphorus which also shows anisotropic electrical and optical properties^{39,40}. Therefore, ReS₂ and ReSe₂ are quasi 1D materials in terms of the low energy hole carrier dynamics, which makes ReS₂ and ReSe₂ promising bulk materials for 1D semiconducting electronics. The effective mass of ReS₂ observed by ARPES is found to be significantly enhanced compared to that from first principles calculations. Electron-electron and electron-phonon interactions or atomic spin-orbit coupling of Re atom may be attributed to the mass enhancement⁴¹. The quasi 1D character of the hole carriers as well as possibility of the electron-electron and electron-phonon interactions may lead to charge density wave order if enough amount of hole carriers are doped into ReS₂ and ReSe₂⁴².

Methods

ARPES measurement. We performed ARPES experiments at the beamline 4.0.3.2 (MERLIN) of the Advanced Light Source at the Lawrence Berkeley National Laboratory equipped with VG-Scienta R8000 electron analyzer. All samples are cleaved *in-situ* and data were taken at 200 K to avoid the charging effect in a vacuum better than 6×10^{-11} Torr. with linearly polarized light. For the k_z dependence experiment, photon energies between 60 and 110 eV with 2 eV energy step were used. The total energy resolution was better than 20 meV with a momentum resolution of 0.004 \AA^{-1} .

References

- Xiao, D., Liu, G.-B., Feng, W. X., Xu, X. & Yao, W. Coupled Spin and Valley Physics in Monolayers of MoS₂ and Other Group-VI Dichalcogenides. *Phys. Rev. Lett.* **108**, 196802 (2012).
- Xu, X., Yao, W., Xiao, D. & Heinz, T. F. Spin and pseudospins in layered transition metal dichalcogenides. *Nat. Phys.* **10**, 343–350 (2014).
- Jones, A. M. *et al.* Spin-layer locking effects in optical orientation of exciton spin in bilayer WSe₂. *Nat. Phys.* **10**, 130–134 (2014).
- Yao, W. *et al.* Direct observation of spin-layer locking by local Rashba effect in monolayer semiconducting PtSe₂ film. *Nat. Commun.* **8**, 14216 (2017).
- Frindt, R. F. Superconductivity in Ultrathin NbSe₂ Layers. *Phys. Rev. Lett.* **28**, 299 (1972).
- Arguello, C. J. *et al.* Visualizing the charge density wave transition in 2H-NbSe₂ in real space. *Phys. Rev. B* **89**, 235115 (2014).

7. Jin, C. H. *et al.* Ultrafast dynamics in van der Waals heterostructures. *Nat. Nanotech.* **13**, 994–1003 (2018).
8. Rivera, P. *et al.* Interlayer valley excitons in heterobilayers of transition metal dichalcogenides. *Nat. Nanotech.* **13**, 1004–1015 (2018).
9. Manzeli, S., Ovchinnikov, D., Pasquier, D., Yazyev, O. V. & Kis, A. 2D transition metal dichalcogenides. *Nat. Rev. Mater.* **2**, 17033 (2017).
10. Wang, G. *et al.* Colloquium: Excitons in atomically thin transition metal dichalcogenides. *Rev. Mod. Phys.* **90**, 021001 (2018).
11. Chhowalla, M. *et al.* The chemistry of two-dimensional layered transition metal dichalcogenide nanosheets. *Nat. Chem.* **5**, 263–275 (2013).
12. Tongay, S. *et al.* Monolayer behavior in bulk ReS₂ due to electronic and vibrational decoupling. *Nat. Commun.* **5**, 3252 (2014).
13. Tiong, K. K., Ho, C. H. & Huang, Y. S. The electrical transport properties of ReS₂ and ReSe₂ layered crystals. *Solid State Commun.* **111**, 635–640 (1999).
14. Wolverson, D., Crampin, S., Kazemi, A. S., Ilie, A. & Bending, S. J. Raman Spectra of Monolayer, Few-layer, and bulk ReSe₂: An Anisotropic Layered Semiconductor. *ACS Nano* **8**, 11154–11164 (2014).
15. Lorchat, E., Froehlicher, G. & Berciaud, S. Splitting of Interlayer Shear Modes and Photon Energy Dependent Anisotropic Raman Response in N-Layer ReSe₂ and ReS₂. *ACS Nano* **10**, 2752–2760 (2016).
16. Chenet, D. *et al.* In-Plane Anisotropy in Mono- and Few-Layer ReS₂ Probed by Raman Spectroscopy and Scanning Transmission Electron Microscopy. *Nano Lett.* **15**, 5667–5672 (2016).
17. He, R. *et al.* Coupling and Stacking Order of ReS₂ Atomic Layers Revealed by Ultralow-Frequency Raman Spectroscopy. *Nano Lett.* **16**, 1404–1409 (2016).
18. Nagler, P., Plenchinger, G., Schüller, C. & Korn, T. Observation of anisotropic interlayer Raman modes in few-layer ReS₂. *Phys. Status Solidi RRL* **10**, 185–189 (2016).
19. Li, L. *et al.* Strong In-Plane Anisotropies of Optical and Electrical Response in Layered Dimetal Chalcogenide. *ACS Nano* **11**, 10264–10272 (2017).
20. Ho, C. H., Huang, Y. S., Tiong, K. K. & Liao, P. C. Absorption-edge anisotropy in ReS₂ and ReSe₂ layered semiconductors. *Phys. Rev. B* **58**, 16130 (1998).
21. Zhong, H.-X., Gao, S. Y., Shi, J.-J. & Yang, L. Quasiparticle band gaps, excitonic effects, and anisotropic optical properties of the monolayer distorted 1T diamond-chain structures ReS₂ and ReSe₂. *Phys. Rev. B* **92**, 115438 (2015).
22. Aslan, O. B., Chenet, D. A., van der Zande, A. M., Hone, J. C. & Heinz, T. F. Linearly Polarized Excitons in Single- and Few-Layer ReS₂ Crystals. *ACS Photonics* **3**, 96–101 (2016).
23. Sim, S. *et al.* Selectively tunable optical Stark effect of anisotropic excitons in atomically thin ReS₂. *Nat. Commun.* **7**, 13569 (2016).
24. Sim, S. *et al.* Ultrafast quantum beats of anisotropic excitons in atomically thin ReS₂. *Nat. Commun.* **9**, 351 (2018).
25. Ho, C. H., Huang, Y. S. & Tiong, K. K. In-plane anisotropy of the optical and electrical properties of ReS₂ and ReSe₂ layered crystals. *J. Alloys Comp.* **317**, 222–226 (2001).
26. Hu, S. Y., Liang, C. H., Tiong, K. K., Huang, Y. S. & Lee, Y. C. Electrical Anisotropy of W-Doped ReSe₂ Crystals. *J. Electrochem. Soc.* **153**, J100–J102 (2006).
27. Biswas, D. *et al.* Narrow-band anisotropic electronic structure of ReS₂. *Phys. Rev. B* **96**, 085205 (2017).
28. Gehlmann, M. *et al.* Direct Observation of the Band Gap Transition in Atomically Thin ReS₂. *Nano Lett.* **17**, 5187–5192 (2017).
29. Webb, J. L. *et al.* Electronic band structure of ReS₂ by high-resolution angle-resolved photoemission spectroscopy. *Phys. Rev. B* **96**, 115205 (2017).
30. Hart, L. S. *et al.* Electronic bandstructure and van der Waals coupling of ReSe₂ revealed by high-resolution angle-resolved photoemission spectroscopy. *Sci. Rep.* **7**, 5145 (2017).
31. Ho, C. H., Huang, Y. S., Liao, P. C. & Tiong, K. K. Crystal structure and band-edge transition of ReS_{1-x}Se_x layered compounds. *J. Phys. Chem. Solids* **60**, 1797–1804 (1999).
32. Arora, A. *et al.* Highly Anisotropic in-Plane Excitons in Atomically Thin and Bulklike 1T'-ReSe₂. *Nano Lett.* **17**, 3202–3207 (2017).
33. Eickholt, P. *et al.* Location of the valence band maximum in the band structure of anisotropic 1T'-ReSe₂. *Phys. Rev. B* **97**, 165130 (2018).
34. Yu, S. *et al.* Strain-engineering the anisotropic electrical conductance in ReS₂ monolayer. *Appl. Phys. Lett.* **108**, 191901 (2016).
35. Kim, B. S., Rhim, J.-W., Kim, B. Y., Kim, C. & Park, S. R. Determination of the band parameters of bulk 2H-MX₂ (M = Mo, W; X = S, Se) by angle-resolved photoemission spectroscopy. *Sci. Rep.* **6**, 36389 (2016).
36. Bovet, M. *et al.* Interplane coupling in the quasi-two-dimensional 1T-TaS₂. *Phys. Rev. B* **67**, 125105 (2003).
37. Miró, P., Audiffred, M. & Heine, T. An atlas of two-dimensional materials. *Chem. Soc. Rev.* **43**, 6537–6554 (2014).
38. Zibouche, N., Philipsen, P., Kuc, A. & Heine, T. Transition-metal dichalcogenide bilayers: Switching materials for spintronic and valleytronic applications. *Phys. Rev. B* **90**, 125440 (2014).
39. Xia, F., Wang, H. & Jia, Y. Rediscovering black phosphorus as an anisotropic layered material for optoelectronic and electronics. *Nat. Commun.* **5**, 4458 (2014).
40. Akahama, Y., Endo, S. & Narita, S.-I. Electrical Properties of Black Phosphorus Single Crystals. *J. Phys. Soc. Jpn.* **52**, 2148–2155 (1983).
41. Mahan, G. D. *Many-Particle Physics* (New York 1990).
42. Grüner, G. *Density Waves in Solids* (New York 1994).

Acknowledgements

This work was supported by the Incheon National University Research Grant in 2014. B.S.K. and C.K. acknowledges the support from research program of Institute for Basic Science (Grant No. IBS-R009-G2).

Author Contributions

B.S.K. and W.S.K. performed ARPES measurements with the support from J.D.D.; B.S.K. analyzed the ARPES data; B.S.K., C.K. and S.R.P. wrote the paper; C.K. and S.R.P. are responsible for project direction and planning.

Additional Information

Supplementary information accompanies this paper at <https://doi.org/10.1038/s41598-019-39540-4>.

Competing Interests: The authors declare no competing interests.

Publisher's note: Springer Nature remains neutral with regard to jurisdictional claims in published maps and institutional affiliations.



Open Access This article is licensed under a Creative Commons Attribution 4.0 International License, which permits use, sharing, adaptation, distribution and reproduction in any medium or format, as long as you give appropriate credit to the original author(s) and the source, provide a link to the Creative Commons license, and indicate if changes were made. The images or other third party material in this article are included in the article's Creative Commons license, unless indicated otherwise in a credit line to the material. If material is not included in the article's Creative Commons license and your intended use is not permitted by statutory regulation or exceeds the permitted use, you will need to obtain permission directly from the copyright holder. To view a copy of this license, visit <http://creativecommons.org/licenses/by/4.0/>.

© The Author(s) 2019